J. Plasma Physics (2011), *vol.* 77, *part* 6, *pp.* 843–855.
doi:10.1017/S0022377811000262

Torsional magnetic reconnection: The effects of localizing the non-ideal (ηJ) term

PETER F. WYPER and REKHA JAIN

School of Mathematics & Statistics, University of Sheffield, Sheffield, UK
(app09pfw@sheffield.ac.uk)

(Received 4 January 2011; accepted 11 May 2011; first published online 13 June 2011)

Abstract. Magnetic reconnection in three dimensions (3D) is a natural extension from X-point reconnection in two dimensions. Of central importance in the 3D process is a localized non-ideal region within which the plasma and magnetic field decouple allowing for field line connectivity change. In practice, localized current structures provide this localization; however, mathematically a similar effect can be achieved with the localization of plasma resistivity instead. Physically though, such approaches are unrealistic, as anomalous resistivity requires very localized currents. Therefore, we wish to know how much information is lost in localizing η instead of current? In this work we develop kinematic models for torsional spine and fan reconnection using both localized η and localized current and compare the non-ideal flows predicted by each. We find that the flow characteristics are dictated almost exclusively by the form taken for the current profile with η acting only to scale the flow. We do, however, note that the reconnection mechanism is the same in each case. Therefore, from an understanding point of view, localized η models are still important first steps into exploring the role of non-ideal effects.

1. Introduction

Magnetic reconnection is a fundamental physical process of many astrophysical plasmas. It is the restructuring of magnetic field through the changing of connectivity of the magnetic field lines. This restructuring allows the release of much of the stored energy in the field. It is this property that makes reconnection attractive as the mechanism responsible for phenomena such as magnetic substorms and solar flares.

In recent years much work has been done to understand this process in three dimensions (3D). In three dimensions reconnection can take place at and around null points in the form of spine-fan (or the degenerate spine and fan cases) and torsional reconnection types (see [1] for a review). It may also occur at separator lines, that is special field lines that connect two null points [2] or without the presence of null points as long as in some region there is a component of electric field parallel to the magnetic field [3].

Of importance in these processes is the localization of the non-ideal term (the product of resistivity η and current density **J**) in Ohm's law. In practice it is the localization of the current structure that provides this (see, for instance, [4], [5]). The localization may also be enhanced by anomalous resistivity generated by microturbulence when the current layer becomes very thin [6]. However, this still depends upon a localized current layer.

In analytical methods, however, the reconnection process can be localized through either η or current. Being a scalar rather than a vector dealing with η is much simpler, thereby often making it the starting point of investigations into 3D non-ideal processes. The local η approach sits a region of localized resistivity in a superconducting plasma threaded with a magnetic field containing a linear or constant current (for example [7]– [9]). Such a scenario is almost unrealizable physically, because although anomalous resistivity is possible, it is created by a very localized current and is anomalous above some background non-zero resistive value.

Despite its drawbacks this method seems to yield most of the important characteristics of processes it is applied to. Therefore, the questions that need to be addressed here are how much information is lost by localizing η instead of $\mathbf{J}$? Are the resulting flows seen driven by the form of η or current chosen? Is the reconnection mechanism really the same? Often there is no local $\mathbf{J}$ model to compare with. In this work we will attempt to address these questions by careful comparison of the flux transport for a reconnection process localized using a local current region and one localized using a localized resistivity. This will be done by extending the models developed in [10] for torsional reconnection to include a localized resistive region.

Section 2 introduces the methodology. Sections 3–5 present our results and Secs 6 and 7 discuss the findings and present our conclusions, respectively.

2. The framework: Steady state magnetohydrodynamics (MHD)

We will work within the kinematic steady state MHD framework such that the equations governing our system are given by

$$\mathbf{E} + \mathbf{v} \times \mathbf{B} = \eta \mathbf{J}, \tag{2.1}$$

$$\nabla \times \mathbf{E} = 0, \tag{2.2}$$

$$\nabla \times \mathbf{B} = \mu_0 \mathbf{J}, \tag{2.3}$$

$$\nabla \cdot \mathbf{B} = 0. \tag{2.4}$$

Equation (2.2) allows us to express the electric field in terms of an electric potential ($\mathbf{E} = -\nabla \Phi$) whose behavior is governed by ideal as well as non-ideal terms. The component of (2.1) parallel to the magnetic field allows us to express these terms explicitly

$$\Phi = -\int \eta \mathbf{J} \cdot \mathbf{Bds} + \Phi_0, \tag{2.5}$$

where $\nabla \Phi_0 \cdot \mathbf{B} = 0$ and $s = \lambda/|B|$, and λ is the distance along a field line. For the rest of this analysis the ideal term Φ_0 is set to zero allowing only non-ideal effects to be apparent. The integral is solved by using the field line equations in (r, ϕ, z) expressed in terms of parameter s and some initial position (r_0, ϕ_0, z_0). The field line equations are obtained by solving

$$\frac{dr}{B_r} = \frac{r d\phi}{B_\phi} = \frac{dz}{B_z} = ds. \tag{2.6}$$

These equations are invertible, so Φ can be represented as a function of s and initial position to carry out the integral in (2.5) and then transferred back into a function

https://doi.org/10.1017/S0022377811000262 Published online by Cambridge University Press

of r, ϕ, and z to find the electric field from

$$\mathbf{E} = -\nabla\Phi. \tag{2.7}$$

Thus, for a given magnetic configuration we can find the electric field due to non-ideal effects (i.e. those due to $\eta\mathbf{J} \neq 0$). Using this we can also find the resulting flow velocity perpendicular to the magnetic field by taking the vector product of (2.1) with $\mathbf{B}$ to give

$$\mathbf{v}_\perp = \frac{(\mathbf{E} - \eta\mathbf{J}) \times \mathbf{B}}{B^2}. \tag{2.8}$$

We see that the product $\eta\mathbf{J}$ appears twice; in (2.5) (and thus, implicitly in $\mathbf{E}$) and (2.8). It is, therefore, interesting to study the flow properties with localized $\eta\mathbf{J}$.

Unless otherwise stated in the rest of this analysis we consider when $B_0 = \mu_0 = \eta_0 = 1$ with vector plots produced using a $(\text{strength}/\max)^{1/d}$ scaling.

3. Torsional spine

Consider the case of localization of the $\eta\mathbf{J}$ product to around the spine. We start with a symmetric linear null point field

$$\mathbf{B}_n = B_0\,(r, 0, -2z), \tag{3.1}$$

to which we add a localized perturbation

$$\mathbf{B}_p = \mu_0 j_0 r^\alpha e^{-\frac{a_1^2 r^2}{l^2}} \hat{\boldsymbol{\phi}}, \tag{3.2}$$

from which we get a localized current density. The field line equations are then given by

$$r = r_0 e^{B_0 s}, \tag{3.3}$$

$$z = z_0 e^{-2B_0 s}, \tag{3.4}$$

$$\phi = \mu_0 j_0 F_{a_1^2}(\alpha - 1) + C, \tag{3.5}$$

where $F_n(A) = \int r^A e^{-\frac{nr^2}{l^2}} ds$ and C is a constant of integration. This is solved by choosing positive integer values for α and using

$$F_n(A+2) = \frac{l^2}{2n}\left(AF_n(A) - \frac{r^A}{B_0} e^{-\frac{nr^2}{l^2}}\right), \tag{3.6}$$

found by applying integration by parts to $F(A)$. We then introduce a localized resistivity with a similar form to $\mathbf{B}_p$,

$$\eta = \eta_0 r^\lambda e^{-\frac{a_2^2 r^2}{l^2}}. \tag{3.7}$$

Then (2.5) gives us the general electric potential for steady state torsional spine reconnection

$$\Phi = j_0 \eta_0 B_0 \left[-\frac{4a_1^2}{l^2} F_p(\alpha + \lambda - 1) + 2(\alpha + 1) F_p(\alpha + \lambda - 3) \right] z r^2, \tag{3.8}$$

where $p = a_1^2 + a_2^2$. We find realistic solutions when $\alpha + \lambda \geqslant 4$ and even, generalizing the previous result when $\lambda = 0$. This condition arises from the necessity that $v_{\perp r} \neq 0$

https://doi.org/10.1017/S0022377811000262 Published online by Cambridge University Press

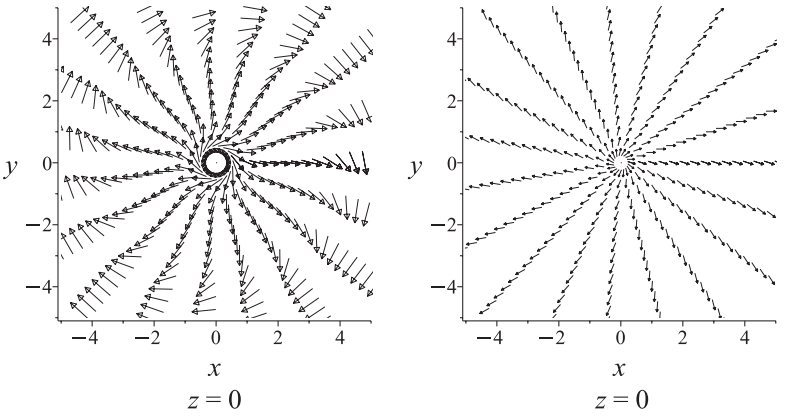

Figure 1. Plasma flow in the fan plane when localization is radial only for $j_0 = 3, l = 1.75$ and $d = 11$. Left: local $\mathbf{J}$ ($\alpha = 4, a_1 = 1, \lambda = a_2 = 0$); right: local η ($\alpha = 1, a_1 = 0$, $\lambda = 3, a_2 = 1$).

except when $r = 0$ to avoid sinks and sources in the flow. In effect this means that $E_z \neq 0$ or as reported in [10], $F(\alpha - 3)/F(\alpha - 1) \neq 2/(\alpha + 1)l^2$. This condition now generalizes to

$$\frac{F(\alpha + \lambda - 3)}{F(\alpha + \lambda - 1)} \neq \frac{2a_1^2}{(\alpha + 1)l^2}. \tag{3.9}$$

Thus, it is the sum of α and λ that must be even. Moreover, we find that the choices of λ that satisfy (3.9) are limited by the relative localization of η to $\mathbf{J}$, i.e. $(a_2/a_1)^2$. For a non-localized $\mathbf{J}$ ($a_1 = 0$) we may use any value of λ as long as $\alpha + \lambda \geqslant 4$ and even. When $\mathbf{J}$ is localized, however, for some choices of λ a degree of η localization is required ($a_2 \neq 0$) to find a realistic solution. For the rest of this analysis we will only consider cases that are well behaved for all values of $(a_2/a_1)^2$.

3.1. Radial localization: Local η ($\mathbf{J}$ constant) vs. local $\mathbf{J}$ (η constant).

We start with direct comparison between flows for a localized current (with η constant) and a localized η (with $\mathbf{J}$ constant). The two cases we consider are when $\alpha = 4, a_1 = 1, \lambda = a_2 = 0$ giving

$$\mathbf{J} = \nabla \times \left(j_0 r^4 e^{-\frac{r^2}{l^2}} \hat{\boldsymbol{\phi}} \right), \quad \eta = \eta_0, \tag{3.10}$$

and when $\alpha = 1, a_1 = 0, \lambda = 3, a_2 = 1$ giving

$$\mathbf{J} = j_0 (0, 0, 1), \quad \eta = \eta_0 r^3 e^{-\frac{r^2}{l^2}}. \tag{3.11}$$

Figure 1 shows the perpendicular plasma flow in the fan plane for the two cases. Both flows are rotational and clockwise in direction. Two factors dominate the nature of the flows: the relative localization and relative power law nonlinearity of η and $\mathbf{J}$. In order to understand better the role of each, we now investigate them separately.

3.1.1. Relative power law nonlinearity: α relative to λ. Consider localizing $\mathbf{J}$ without localizing η, i.e set $a_1 = 1, a_2 = 0$ for various combinations of α and λ such that

https://doi.org/10.1017/S0022377811000262 Published online by Cambridge University Press

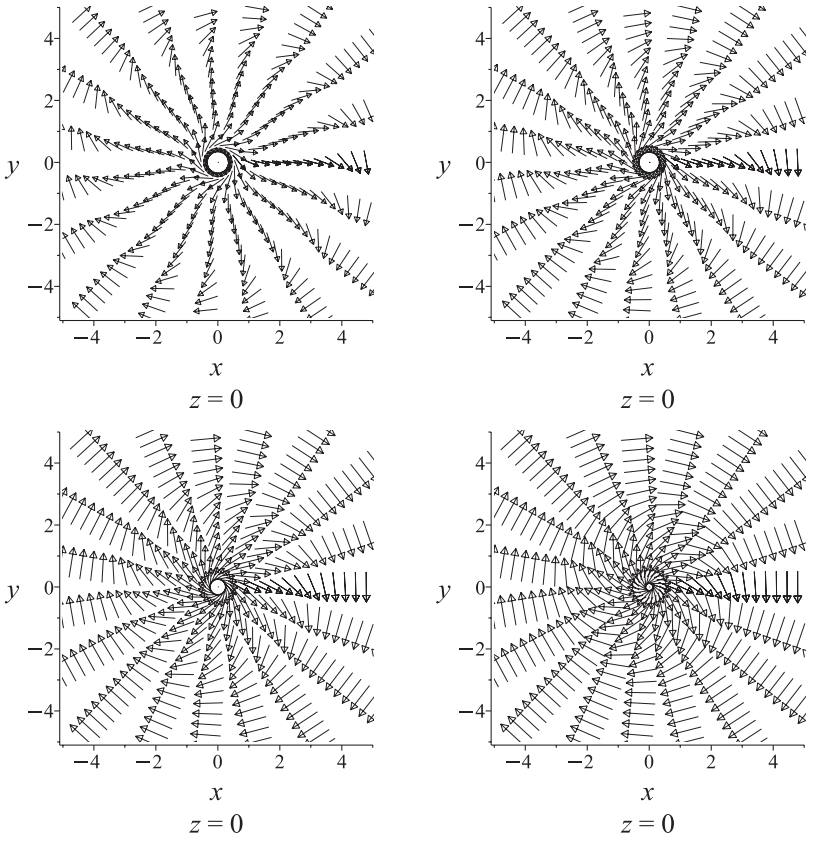

Figure 2. Plasma flow in the fan plane when localization is radial only with $a_1 = 1, a_2 = 0, j_0 = 3, l = 1.75$ and $d = 11$ for various combinations of $\alpha + \lambda = 4$. Top left $\alpha = 4, \lambda = 0$ (constant η); top right $\alpha = 3, \lambda = 1$; bottom left $\alpha = 2, \lambda = 2$; bottom right $\alpha = 1, \lambda = 3$ (constant $\mathbf{J}$ along spine).

$\alpha + \lambda = 4$,

$$\mathbf{J} = \nabla \times \left(j_0 r^{\alpha} e^{-\frac{r^2}{l^2}} \hat{\boldsymbol{\phi}} \right), \quad \eta = \eta_0 r^{\lambda}. \tag{3.12}$$

Figure 2 marks the progression from a strongly nonlinear current to a constant current along the spine. We see that as the nonlinearity in $\mathbf{J}$ is decreased the relative amount of outflow to rotation follows. This pattern is also apparent when $\alpha + \lambda \neq 4$ and even but care with the relative values of a_1 and a_2 must be taken to find realistic flows. So it appears that it is the nonlinearity of $\mathbf{J}$ that dictates the flow topology. Is this the case for current localization also?

3.1.2. Relative localization: a_1 relative to a_2. Consider a nonlinear current and an η that is constant along the spine, i.e. set $\alpha = 4, \lambda = 0$. We can vary the radial localization of such η and $\mathbf{J}$ through choices of a_1 and a_2

$$\mathbf{J} = \nabla \times \left(j_0 r^4 e^{-\frac{a_1^2 r^2}{l^2}} \hat{\boldsymbol{\phi}} \right), \quad \eta = \eta_0 e^{-\frac{a_2^2 r^2}{l^2}}. \tag{3.13}$$

https://doi.org/10.1017/S0022377811000262 Published online by Cambridge University Press

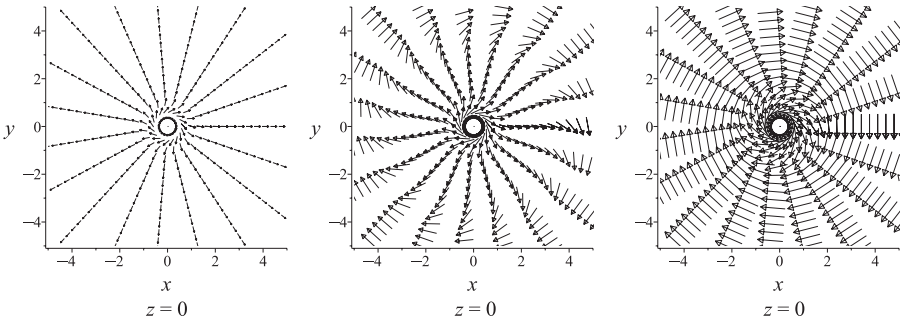

Figure 3. Localized η case ($a_2 = 1$) with $j_0 = 3, l = 1.75$ and $d = 11$ when $\alpha = 4$ and $\lambda = 0$. Illustrated is the plasma flow in the fan plane when current localization is gradually increased. Left: $a_1 = 0$; middle: $a_1 = 1$; right: $a_1 = 2$.

Figure 3 shows how, keeping η localized ($a_2 = 1$), as we increase the current localization (a_1) the region of strong outflow (relative to rotation) controlled by the power law dependence of $\mathbf{J}$ is localized by the edge of the current region (i.e. the region where $|\mathbf{J}| \ll |\mathbf{J}|_{\max}$ here sitting beyond some radius R). Outside the current region the flow is predominantly rotational. Once $\mathbf{J}$ is localized if we turn off the η localization by setting $a_2 = 0$ there is no change in the flow topology, only a scaling up of magnitude where the plasma η is now greater. Thus, again it is the form of $\mathbf{J}$ that dictates the topology of the plasma flow and therefore how flux is moved around within the system. In this case η only acts to scale up or down the magnitude of flow.

4. Torsional fan

Consider when the $\eta\mathbf{J}$ term is localized to near the fan plane. In this case the local field perturbation takes the form

$$\mathbf{B}_p = \mu_0 j_0 r z^\gamma e^{-\frac{b_1^2 z^2}{l^2}} \hat{\boldsymbol{\phi}}. \tag{4.1}$$

This has a linear dependence on r to avoid singular currents. The field lines for this field are described by

$$r = r_0 e^{B_0 s}, \tag{4.2}$$

$$z = z_0 e^{-2B_0 s}, \tag{4.3}$$

$$\phi = \mu_0 j_0 G_{b_1^2}(\gamma) + C, \tag{4.4}$$

where C is a constant of integration and $G_m(A) = \int z^A e^{-\frac{mz^2}{l^2}} ds$. This is solved by choosing positive integer values for γ and using

$$G_m(A+2) = \frac{l^2}{2m}\left(AG_m(A) + \frac{z^A}{2B_0} e^{-\frac{mz^2}{l^2}}\right), \tag{4.5}$$

found by applying integration by parts to $G(A)$. After introducing resistivity with a similar form to $\mathbf{B}_p$,

$$\eta = \eta_0 z^\delta e^{-\frac{b_2^2 z^2}{l^2}}, \tag{4.6}$$

https://doi.org/10.1017/S0022377811000262 Published online by Cambridge University Press

(2.5) gives the general electric potential for steady state torsional fan reconnection,

$$\Phi = j_0\eta_0 B_0\left[\left(\gamma G_q(\gamma+\delta-2) - \frac{2b_1^2}{l^2}G_q(\gamma+\delta)\right)zr^2 + 4G_q(\gamma+\delta+1)\right], \tag{4.7}$$

where $q = b_1^2 + b_2^2$. We find realistic solutions when $\gamma + \delta \geqslant 3$ and odd, generalizing the previous result when $\delta = 0$ [10]. This condition arises from the necessity that $v_{\perp z} \neq 0$ except when $z = 0$, to avoid sinks and sources in the flow. In effect this means that $E_r \neq 0$ and therefore

$$\frac{G(\gamma+\delta-2)}{G(\gamma+\delta)} \neq \frac{2b_1^2}{\gamma l^2}. \tag{4.8}$$

Thus, it is the sum of γ and δ that must be odd. Like the torsional spine case choices of δ that satisfy (4.8) are limited by the relative localization of η to $\mathbf{J}$, in this case $(b_2/b_1)^2$. The use of δ is further limited to *even* values so that η remains symmetric. Therefore, since $\gamma + \delta \geqslant 3$ for realistic solutions $\gamma \geqslant 1$ and odd. For the rest of this analysis we again consider only cases that are well behaved for all values of $(b_2/b_1)^2$.

4.1. Vertical localization: Local η ($\mathbf{J}$ constant) vs. local $\mathbf{J}$ (η constant)

We begin again with the direct comparison between a local η model (with $\mathbf{J}$ constant) and a local $\mathbf{J}$ model (with η constant). The two cases we will consider are when $\gamma = 3, b_1 = 1$ and $\delta = b_2 = 0$ giving

$$\mathbf{J} = \nabla \times \left(j_0 r z^3 e^{-\frac{z^2}{l^2}}\hat{\boldsymbol{\phi}}\right), \quad \eta = \eta_0, \tag{4.9}$$

and when $\gamma = 1, b_1 = 0$ and $\delta = 2, b_2 = 1$ giving

$$\mathbf{J} = j_0(-r, 0, 2z), \quad \eta = \eta_0 z^2 e^{-\frac{z^2}{l^2}}. \tag{4.10}$$

Figure 4 shows the perpendicular plasma flow in the xy-plane at various heights above the fan plane for each case. As in the torsional spine case, there are slight differences here too but due now to the nonlinearity and relative localization of η and $\mathbf{J}$ in z.

4.1.1. Relative power law non-linearity: γ relative to δ. Consider localizing η in height without localizing $\mathbf{J}$, i.e. set $b_2 = 1, b_1 = 0$ for various combinations of γ and δ such that $\gamma + \delta = 5$,

$$\mathbf{J} = \nabla \times \left(j_0 r z^\gamma \hat{\boldsymbol{\phi}}\right), \quad \eta = \eta_0 z^\delta e^{-\frac{z^2}{l^2}}. \tag{4.11}$$

Figure 5 shows the progression from a strongly nonlinear current to a linear one when $|z| > 1$ and $|z| < 1$. We see that above $z = 1$ an increase in nonlinearity of $\mathbf{J}$ increases the relative amount of outflow to rotation whereas below $z = 1$ the trend is reversed.

Generally the influence of $\mathbf{J}$ is enhanced by increasing γ. When $|z| > 1$ this produces a positive effect but when $|z| < 1$ the smallness of $\mathbf{J}$ is excenuated and the effect is negative. Therefore like the torsional spine case we see that the relative amount of outflow to rotation is controlled by the nonlinearity of $\mathbf{J}$.

https://doi.org/10.1017/S0022377811000262 Published online by Cambridge University Press

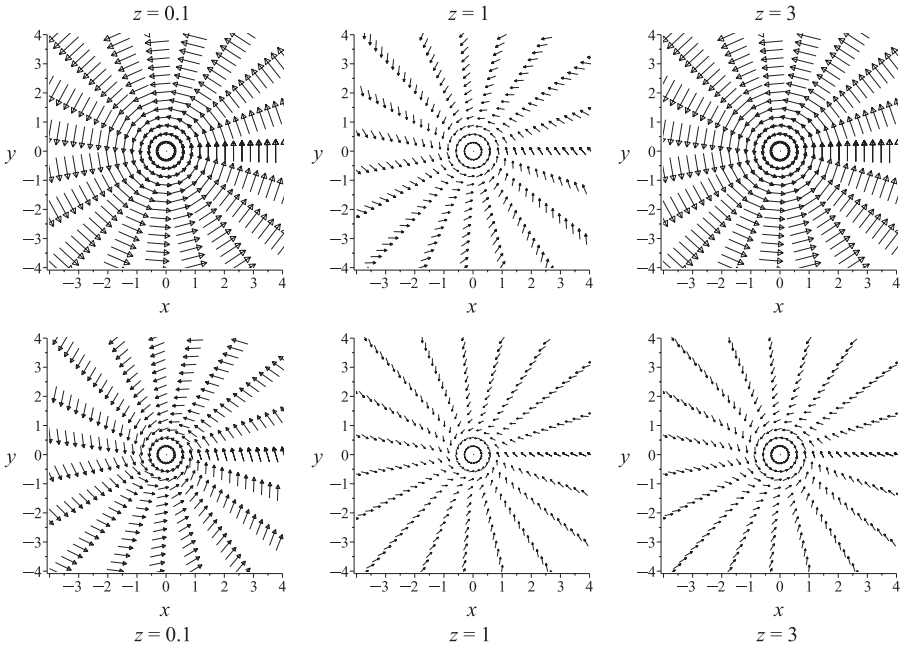

Figure 4. Plasma flow at various heights within the $\eta\mathbf{J}$ layer when the localization is in height only with $j_0 = 3, l = 1$ and $d = 3$. Top row: local $\mathbf{J}$ ($\gamma = 3, \delta = 0, b_1 = 1, b_2 = 0$); bottom row: local η ($\gamma = 1, \delta = 2, b_1 = 0, b_2 = 1$).

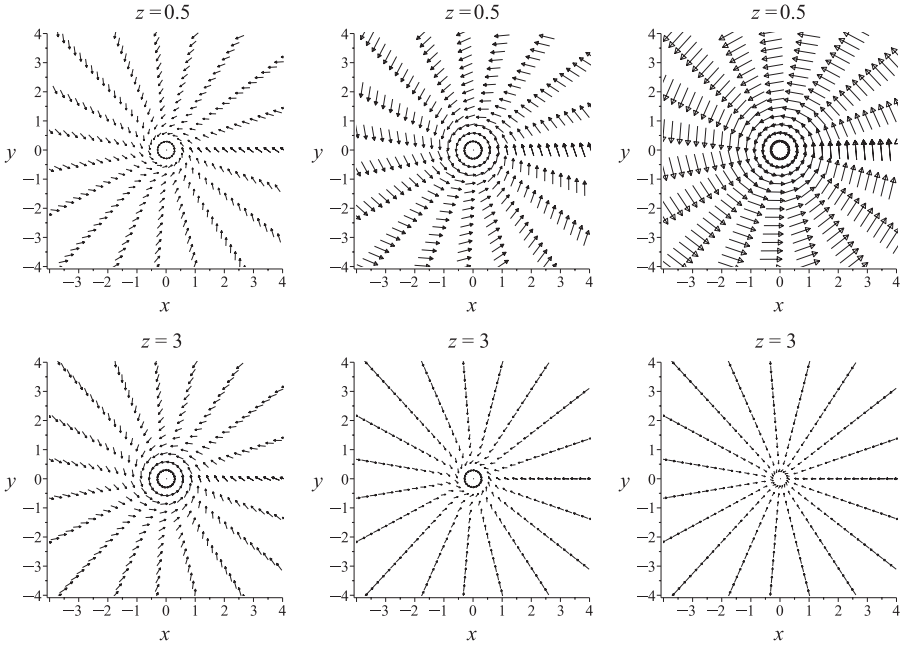

Figure 5. Plasma flow in the xy-plane for vertical localization only with $j_0 = 3, l = 1$ and $d = 3$. Plotted for various combinations of $\gamma + \delta = 5$ with η localized ($b_2 = 1$) and $\mathbf{J}$ not ($b_1 = 0$). Left: $\gamma = 1, \delta = 4$, middle: $\gamma = 3, \delta = 2$, right: $\gamma = 5, \delta = 0$.

https://doi.org/10.1017/S0022377811000262 Published online by Cambridge University Press

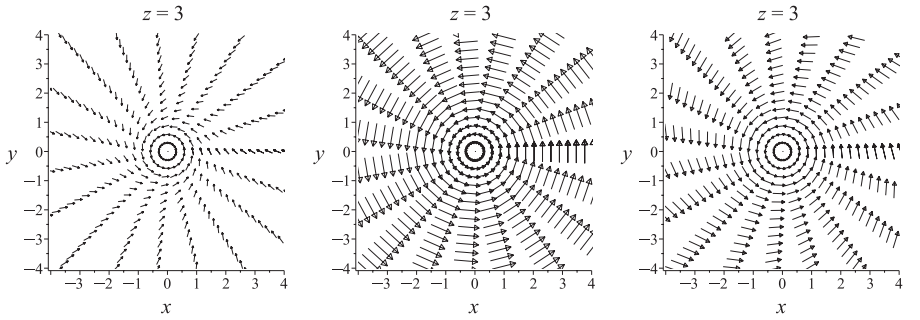

Figure 6. Plasma flow in the $z = 3$ plane when current localization is increased (b_1) for a localized η ($b_2 = 1$) with $j_0 = 3, l = 1, d = 3$ and $\gamma = 1, \delta = 2$. Left: $b_1 = 0$, middle: $b_1 = 0.5$, right: $b_1 = 1$.

4.1.2. Relative localization: b_1 relative to b_2. Consider a current that is linear in r in the fan plane and a nonlinear η, i.e. set $\gamma = 1, \delta = 2$,

$$\mathbf{J} = \nabla \times \left(j_0 r z e^{-\frac{b_1^2 z^2}{l^2}} \hat{\boldsymbol{\phi}} \right), \quad \eta = \eta_0 z^2 e^{-\frac{b_2^2 z^2}{l^2}}. \tag{4.12}$$

We vary the vertical localization of each through choices of b_1 and b_2. In Fig. 6 we see that, keeping η localized ($b_2 = 1$), increasing the current localization (b_1) increases the relative rotation to outflow. Further, careful investigation reveals the region of increased rotational flow at the edge of the current layer (at some height H where $|\mathbf{J}| \ll |\mathbf{J}|_{\max}$), moving down in height through the $z = 3$ plane as the current layer is further localized (and H reduced). Such a region of increased rotation at the edge of the current layer was also present in the torsional spine case beyond some radius (R) that depended on the localization of $\mathbf{J}$. Therefore, we again confirm that the form of $\mathbf{J}$ plays an important role on the flow topology with η acting only to alter the magnitude of the flow.

5. Field line localization

Consider a magnetic field perturbation localized through the exponential term to the shape of the field lines,

$$\mathbf{B}_p = \mu_0 j_0 r^\alpha z^\gamma (z r^2)^\beta e^{-\frac{c_1^2}{l^2}(z r^2)^2} \hat{\boldsymbol{\phi}}. \tag{5.1}$$

When α and γ are non-zero this perturbation is not localized. For full localization additional exponential factors are needed, i.e. $e^{-\frac{r^2}{l^2}}$ or $e^{-\frac{z^2}{l^2}}$. Indeed this was the approach used in [10] for a constant η. However, in the present context we only wish to study the differences in the flows between local η and local $\mathbf{J}$ models. For this purpose the above simpler form of $\mathbf{B}_p$ is sufficient. The field lines are described

https://doi.org/10.1017/S0022377811000262 Published online by Cambridge University Press

by

$$r = r_0 e^{B_0 s}, \tag{5.2}$$

$$z = z_0 e^{-2B_0 s}, \tag{5.3}$$

$$\phi = \frac{\mu_0 j_0}{B_0(\alpha - 2\gamma - 1)} r_0^{\alpha-1} z_0^{\gamma} (z_0 r_0^2)^{\beta} e^{-\frac{c_1^2}{l^2}(z_0 r_0^2)^2} e^{B_0(\alpha-2\gamma-1)s} + C. \tag{5.4}$$

Taking resistivity with the form

$$\eta = \eta_0 r^{\lambda} z^{\delta} (zr^2)^{\kappa} e^{-\frac{c_2^2}{l^2}(zr^2)^2}, \tag{5.5}$$

and combining it with $\mathbf{J}$ in (2.5) we find the electric potential

$$\Phi = j_0 \eta_0 \left[\left(\gamma + \beta - \frac{2c_1^2}{l^2}(zr^2)^2 \right) \frac{rz^{-1}}{D_1} + 2\left(\alpha + 2\beta + 1 - \frac{4c_1^2}{l^2}(zr^2)^2 \right) \frac{r^{-1}z}{D_2} \right] \tag{5.6}$$

$$\times\ r^{\alpha+\lambda} z^{\gamma+\delta} (zr^2)^{\beta+\kappa} e^{-\frac{c_1^2+c_2^2}{l^2}(zr^2)^2},$$

where $D_1 = \alpha + \lambda - 2(\gamma + \delta) + 3$ and $D_2 = \alpha + \lambda - 2(\gamma + \delta) - 3$. This potential creates flows that are unstable to sinks and sources when the sign of both terms are different. As such to find realistic solutions, we choose our constants either, so that

$$\alpha + \lambda - 2(\gamma + \delta) + 3 > 0 \quad \text{and} \quad \alpha + \lambda - 2(\gamma + \delta) - 3 > 0,$$

making Φ overall positive or so that

$$\alpha + \lambda - 2(\gamma + \delta) + 3 < 0 \quad \text{and} \quad \alpha + \lambda - 2(\gamma + \delta) - 3 < 0,$$

making it negative. It is interesting to note that when $\gamma = \delta = 0$ we recover the condition $\alpha + \lambda \geqslant 4$ found for torsional spine if we insist Φ is positive and when $\alpha = 1, \lambda = 0$ we recover the condition $\gamma + \delta \geqslant 3$ found for torsional fan if we insist that Φ is negative. As in these models the electric field dominates the flow topology, this goes some way to explaining why the flow directions for torsional spine and fan are opposite.

5.1. *Field line localization: Local η ($\mathbf{J}$ constant) vs. local $\mathbf{J}$ (η constant)*

Let us now compare the flows for $\eta\mathbf{J}$ localized to the field lines. We will compare when $\alpha = 4, \beta = 2, c_1 = 0.4, \lambda = \kappa = c_2 = \gamma = \delta = 0$ giving

$$\mathbf{J} = \nabla \times \left(j_0 r^4 (zr^2)^2 e^{-\frac{c_1^2}{l^2}(zr^2)^2} \hat{\boldsymbol{\phi}} \right), \quad \eta = \eta_0, \tag{5.7}$$

and when $\alpha = 1, \lambda = 3, \kappa = 2, c_2 = 0.4, \beta = c_1 = \gamma = \delta = 0$ with resulting current and diffusion region of the form

$$\mathbf{J} = j_0 (0, 0, 1), \quad \eta = \eta_0 r^3 (zr^2)^2 e^{-\frac{c_2^2}{l^2}(zr^2)^2}. \tag{5.8}$$

Considering the form of $\eta\mathbf{J}$ for the first case we expect a band of oppositely directed flow in accordance with the findings of [10]. For the second case the findings of Secs 3.1 and 4.1 suggest a simple scaling down of the flow with no oppositely directed regions.

Figure 7 shows the side on view of the plasma flow for both cases. For the localized current case we find the band of oppositely directed flow as expected with

https://doi.org/10.1017/S0022377811000262 Published online by Cambridge University Press

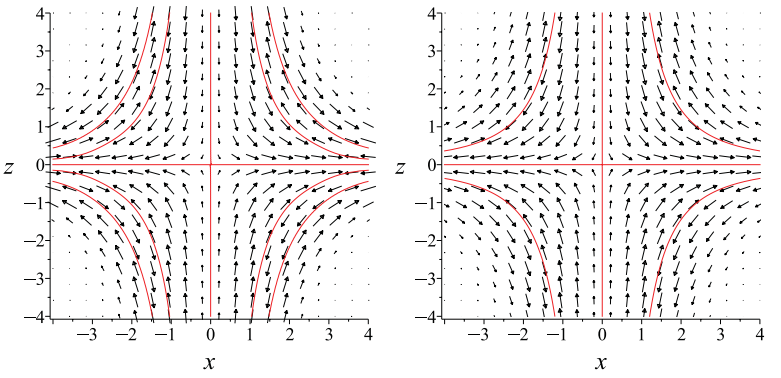

Figure 7. (colour online) Side on view of the plasma flow (symmetric about $r = 0$) when (left panel) **J** is localized to the field lines with a constant η ($c_1 = 0.4, \beta = 2, \alpha = 4, c_2 = \lambda = \kappa = \gamma = \delta = 0$), and when (right panel) η is localized to the field lines with **J** constant ($c_2 = 0.4, \kappa = 2, \alpha = 1, \lambda = 3, c_1 = \beta = \gamma = \delta = 0$). Plots for $j_0 = 3, l = 1.75$ and $d = 21$ with red lines indicating $v_{\perp r} = 0$.

the strongest flow in the region of the strongest current. Surprisingly, however, we see the localized η case also has an oppositely directed flow existing as an infinitely wide region rather than in a discrete band but with the strongest flow still within the region of localized η**J**. Thus, localizing η introduces a topological feature of the localized current flow. In general, when both η and **J** have some degree of field line localization ($c_1 \neq 0, c_2 \neq 0$) we find a discreet band with a width dependent on the localization of **J** , (c_1). As in the cases of radial and vertical localization discussed in Secs 3.1 and 4.1 the relative outflow to rotation in the flow is controlled by the nonlinearity of **J**.

Thus, we find that localizing η gives some flavor of the equivalent localized **J** solution but the flow topology is still dictated by the form of current chosen.

6. Discussion

Generally we see that in these models differences in the flow when η or **J** are localized are driven by differences in the relative localization and relative power law nonlinearity of the chosen forms of η and **J**. This should be expected as it is the competition between power law and exponential decay that creates and controls the localization of each quantity.

In the cases of radial and vertical localization we saw that η acts only as a scaling factor to the magnitude of a flow topology dictated by the form taken for the current profile. In this case when we use a local η with a constant or linear current, effects seen in the equivalent localized current case (here the rotating flow at the edge of the current region) are infinitely far from the null (this is to be expected as $a_1 = b_1 = 0$ is equivalent to $l \to \infty$ in $\mathbf{B}_p$). The flow inside the current region (be it infinite or localized) is dominated by the behavior of the power law but crucially still by the current.

For the field line localization we surprisingly find that when using a localized η, the plasma flow is not simply scaled down but that the topology is altered. Using a localized η in this case introduces a topological feature (the counter rotating

https://doi.org/10.1017/S0022377811000262 Published online by Cambridge University Press

region) of the equivalent localized **J** case. However, this region is a necessity of the transition from radial to height localization. In [10] and again in this work we have seen that the flow direction of torsional fan is oppositely directed in relation to those seen for torsional spine. As discussed in detail in [10], this leads to distinct regions of both flow types in more general perturbations (those with both r and z nonlinearity). That we see distinct regions in models with a localized η and simple **J** merely indicates that the reconnection process is the same as that seen in the case of equivalent localized **J**.

Focusing on the other changes to the flow topology we saw that the infinite counter rotating region (when η is localized for a constant **J**) becomes a discrete band when **J** is also localized ($c_1 \neq 0$). We saw that the outer edge of the band resides on the outer edge of the current region and gets moved in with it as the current is further localized. In addition, the relative outflow to rotation is also controlled by the nonlinearity of **J**. Thus, the flow topology is mainly dictated by the profile of the current density.

7. Conclusion

In general we surmise that although localization of the η**J** product using a localized η can localize a non-ideal region and its associated plasma flow to around the null point, it is a situation very dependent upon the form of current chosen. Effects from localizing the current are not seen fully in local η models, although these models can still give an insight into the topological aspects of the equivalent local **J** model. Topology aside, however, it is clear that the reconnection mechanism remains the same for either approach and therefore from an understanding point of view localized η models are still an important first step into exploring the role of non-ideal effects.

Acknowledgments

P. W. was supported in this work by an EPSRC (UK) studentship.

References

[1] Pontin, D. I. and Priest, E. R. 2009 Three-dimensional null point reconnection regimes. *Phys. Plasmas* **16**, 122101.

[2] Priest, E. R. and Titov, V. S. 1996 Magnetic reconnection at three-dimensional null points. *Phil. Trans. R. Soc. Lon.* A **354**, 2951–2992.

[3] Hesse, M. and Schindler, K. 1988 A theoretical foundation of general magnetic reconnection. *J. Geophys. Res.* **93**, 5559–5567.

[4] Pontin, D. I., Bhattacharjee, A. and Galsgaard, K. 2007 Current sheet formation and non-ideal behavior at three-dimensional magnetic null points. *Phys. Plasmas* **14** 052106.

[5] Pontin, D. I. and Galsgaard, K. 2007 Current amplification and magnetic reconnection at a three-dimensional null point: Physical characteristics. *J. Geophys. Res.* **112**, 3103.

[6] Priest, E. and Forbes, T. 2000 *Magnetic Reconnection.* Cambridge, UK: Cambridge University Press.

[7] Gunnar, H. and Priest E. Evolution of magnetic flux in an isolated reconnection process. *Phys. Plasmas* **10**, 2712–2721

[8] Pontin, D. I., Hornig, G. and Priest, E. R. 2004 Kinematic reconnection at a magnetic null point: Spine-aligned current. *Geophys. Astrophys. Fluid Dyn.* **98**, 407–428.

[9] Pontin, D. I., Hornig, G. and Priest, E. R. 2005 Kinematic reconnection at a magnetic null point: Fan-aligned current. *Geophys. Astrophys. Fluid Dyn.* **99**, 77–93.

[10] Wyper, P. F. and Jain, R. 2010 Torsional magnetic reconnection at 3D null points: A phenomenological study. *Phys. Plasmas.* **17**, 092902.